中國機械工程學刊第四十五卷第三期第 237~251 頁(民國一百一十三年)
Journal of the Chinese Society of Mechanical Engineers, Vol.45, No.3, pp237~251 (2024)

Development of the Airtightness Experimental Device for Diving Suit

Guoqing Gong*, Youmin Wang*and Peng Gong*

Keywords: Diving Suit Airtightness; Pneumatic Servo Control; Mathematical Model; PID Control

ABSTRACT

At the present time, the airtightness testing method of diving devices is comparatively backward, with complicated and inefficient operation of testing devices, which has failed to ensure the airtightness of each diving suit. Regarding the fundamental research and development of the diving suit airtightness testing device, this paper determined the control scheme with the clamping force servo control as the core, drew the 3D model of the clamping and sealing module of the airtightness testing device by means of Solidworks, while conducting ANSYS analysis for the primary force components. Secondly, the mathematical model of the pneumatic servo control system of the diving suit airtightness testing test device was established, while the servo control system of the diving suit airtightness testing test device was analyzed by means of Matlab. It was determined that the stability of the servo control system of this testing experiment device was excellent. Upon the pole configuration, the performance of the pneumatic servo system of the diving suit airtightness testing test device was significantly enhanced, in which the overshoot and stabilization time of the pneumatic servo control system of the diving suit airtightness testing test device were significantly shortened following the introduction of PID control. Lastly, this paper completed the study of airtightness testing methods, determined the testing scheme of diving suit airtightness testing test device by applying the testing principle of direct pressure testing method, in addition to making the design of the control program of PLC in accordance with the whole testing process.

Paper Received September 2023. Revised October 2023. Accepted November 2023. Author for Corresponding: Guoqing Gong

* *Graduate Student, School of Mechanical Engineering, Anhui Polytechnic University, Wuhu, Anhui 241000, China.*

** *Professor, School of Mechanical Engineering, Anhui Polytechnic University, Wuhu, Anhui 241000, China.*

INTRODUCTION

Diving gear refers to the collective term for all the devices worn on the body of the divers to accommodate the underwater environment. Diving gear typically involves a diving rebreather, a diving suit and its accessories. The primary structure of the diving gear contains hard helmet, diving suit, waist joint valve and so forth. Its principal function is to deliver water insulation for divers to operate or exercise underwater, so as to protect their safety underwater. For the sake of verifying whether the diving suit after the completion of production is equipped with excellent performance of waterproof and gas storage to safeguard the safety of divers underwater, the airtightness of the diving suits must be tested prior to entering the market.

Liu et al. (2019) proposed an air tightness detection scheme based on carbon dioxide gas sensor. The adaptive weighted fusion algorithm is used to fuse the weighted data collected by multiple carbon dioxide sensors to compensate the test error of a single sensor. This method is applied to the leak detection of tracer gas with high precision and wide range, and can meet the needs of production. Seigo Goto et al. (2019) proposed a predictive fuzzy control method for pneumatic servo system based on neural network. Using the proposed method, fictional plants are used to predict the future output of plants in the predictive fuzzy scheme. The error between the expected value and the output of the hypothetical factory and the change of the error are applied as the input signal of the predictive fuzzy controller to generate a direct control input. Benarab Amina et al. (2022) discussed some extensions of pole assignment method to linear systems described by delay differential equations. Among them, the methods of finite spectrum allocation, continuous pole placement and partial pole placement are proposed and explained by some simple low-order dynamic systems. Dwarkoba P. Gaikwad et al. (2022) proposed a fine-tuning PID controller for air suspension system, and advanced genetic algorithm is used for parameter tuning of PID controller. They carried out simulation-based experiments, and in the experimental results, they used the proposed method to obtain very small IAE, ISE and ITAE values. The results show that the proposed PID design method has better performance than the other three optimization-based PID design methods and other existing methods. Tong et al. (2023) designed a water level sensor air tightness detector based on STM32. The detector adopts the method of direct pressure gas leak detection, takes STM32F030R8 as the control core, controls the air pump to inflate, the pressure sensor detects the air pressure and outputs the differential signal through the bridge, and the high-precision air pressure measurement module measures the output of the bridge signal. The steps of pressurization, voltage stabilization, load preservation, judgment and output of the air tightness test are realized by program control, and the judgment results are displayed by LCD and output by relay. Liao et al. (2022) proposed a mobile detection method for air tightness of pressure vessels based on piezoelectric pressure sensor. The piezoelectric pressure sensor is used to detect the gas jet produced at the leak of the pressure vessel, which overcomes the selectivity of the testing instrument to the gas medium, and the sensor can be used to approach the outer surface of the pressure vessel wall and the real-time calculation ability of the instrument. the sensitivity of air tightness detection and the accuracy of leak location are improved. Dang et al. (2020) used Siemens S7-1200 PLC for control, cylinders and vacuum generators as actuators, and electrical control through HMI touch screen and relays to achieve the process of automatic positioning and vacuuming of the tested plastic bottles, which greatly improved the testing efficiency and saved labour costs. Jiang et al. (2021) designed a fuzzy-PID control algorithm to control the internal pressure fluctuation of the object to be measured in the air-tightness detection pressure system. The fuzzy controller is added to the conventional PID control, and the fuzzy controller is designed by fuzzifying trigonometric function, product inference rules and center of gravity defuzzification. The correction amount of on-line real-time tuning is added to the initial value of PID, which is used as the input parameter of PID controller, which improves the dynamic and static performance of the nonlinear control system of air tightness detection pressure.

The above-mentioned literature has all failed to carry out the overall design of the airtightness device and force analysis. For this reason, this paper established the overall scheme of airtightness test in accordance with the airtightness test procedure of diving, designed the clamping and sealing structure, as well as the overall structure of the airtightness testing device, followed by conducting force analysis of the principal force components with ANSYS. The mathematical model of the pneumatic servo control system was established, while MATLAB was employed to analyze the model, concluding that the pneumatic servo system was stable. The force servo control system of the diving suit airtightness test device was modeled and simulated by employing simulink, resulting in the step response curve of the system. Meanwhile, the pole configuration and PID algorithm were employed to optimize the system, concluding that the performance of the system was significantly optimized following the introduction of PID. Lastly, the airtightness testing scheme of the diving suit was designed, with the common direct pressure method selected, thereby completing the programming of the PLC.

DESIGN OF DIVING SUIT AIRTIGHTNESS TEST BENCH

The research and development of the test device in this paper was conducted on the basis of pneumatic servo control system, while the overall scheme of the diving airtightness testing test device was presented from the development direction of today's pneumatic servo control technology and intelligent control system for sealing. The airtightness testing device of this diving suit is comprised of four parts. It is illustrated in Figure 1.

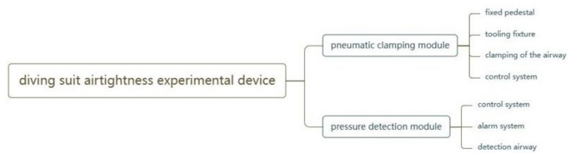

Fig. 1 Composition Diagram of the Airtightness Testing Device of Diving Suit

Pneumatic Circuit Design for Testing Platform

The air tightness testing process in accordance with the diving suit is illustrated in Figure 2, which involves the following two processes.

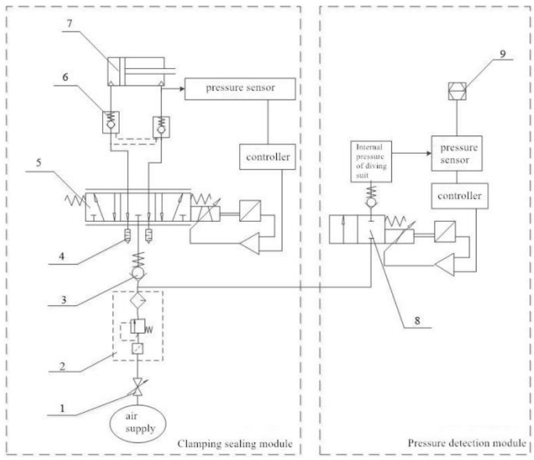

1- Gate Valve; 2- Pneumatic Triplex; 3- Check Valve; 4- Silencer;
2- Three Bit Five Pass Proportional Valve; 6- Pilot Check Valve;
3- 7- Single Rod Double Acting Cylinder; 8- Two Bit Two Pass Solenoid Valve; 9- Computer

Fig. 2 Servo System Diagram for Airtightness Testing

When the right position of the three bit five pass proportional servo valve is connected, the clamping cylinder moves to the left and propels the clamping device to clamp the collar to realize the sealing of the diving suit. After the sealing is completed, the three bit five pass proportional servo valve is not powered on both sides, the cylinder stops moving and the two bit two pass solenoid valve is powered, which makes the diving suit start to inflate. When the air pressure inside the diving suit reaches 0.01MPa, the inflation circuit is closed, after which the pressure inside the diving suit is measured and collected by a pressure sensor, which is transmitted to the display device. If the reduction level of air pressure in the specified time is lower than the set standard, it will issue a warning to remind the detectors. Upon completion of the test, the left side of the three bit five pass proportional servo valve is powered, which propels the cylinder piston cylinder to move outward, while releasing the air pressure inside the diving suit, followed by removing the diving suit after the cylinder movement stops.

Design of Clamping and Sealing Module

The design of the clamping and sealing module primarily involves the design of the upper and lower sealing structure, the design of the support structure, and the design of the guide slot mechanism, as shown in Figure 3, which is a schematic diagram of the diving suit.

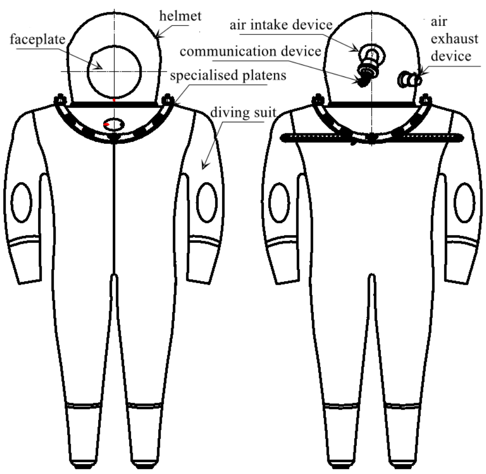

Fig. 3 Schematic Diagram of Diving Suit

(1) Structural Design of Upper and Lower Sealing Plates

In accordance with the shape characteristics of the collar, it is evident that the sealing part requires the adoption of two movable clamping plates, one placed inside the collar and the other clamping with the rubber of the collar part of the suit, so as to realize the clamping and sealing of the collar of the diving suit. Since the cylinder requires installation in the upper sealing plate, the cylinder is installed through the opening of a hole in the upper plate. According to the cylinder model, it can be obtained that the size of the cylinder piston rod is φ25mm, while a hole of φ26mm is opened in the central position of the upper plate for mounting the cylinder. Since the experiment requires the operation of inflating and deflating the diving suit, and the pressure of the gas filled in the suit requires measurement, it was decided in this design to process two holes on the face of the upper sealing plate for inlet and outlet. The left hole in Figure 4 is the inlet hole, and the right hole is the outlet hole, which are connected to the bleed valve and the air pressure detection device for pressure measurement during the pressure holding test.

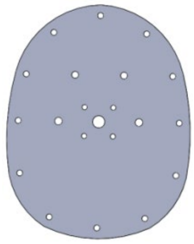

Fig. 4 Upper Sealing Plate

(2) Design of Lower Sealing Plate and Support Structure

For the sake of the reliable sealing effect of the two plates when the cylinder is clamped, the outer contour size of the lower plate surface should be ensured to be the identical with the upper plate. With reference to the original sealing device structure, the clamping force required to seal the two plates is made available by multiple sets of bolts around the plate surface, which in turn makes the lower plate surface a hollow ring-shaped structure.

Upon consideration of the weight of the upper and lower sealing plates and the installation method, it is necessary to add a force support device to the lower plate, to take advantage of the support device to support the cylinder, while also transferring the clamping force of the cylinder uniformly to the positioning nails around the plate surface for the seal of the diving suit, in addition to balancing the radial force of the piston rod through the guide groove. In accordance with the contour form of the lower plate surface and the actual operation requirements, the cross-support method was selected with simple structure and user-friendly operation. As illustrated in Figure 5, the width of the cross-support structure is 40mm, while taking into account the possible deformation generated by the center of the cross-support under force, the four jaws of the cross-support structure are now processed with the bend as illustrated in the figure.

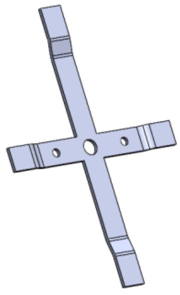

Fig. 5 Cross-support 3D Diagram

The positioning pin of 8mm diameter was installed in the identical position of the bolt hole of the original lower sealing plate (namely the identical position with the positioning hole of the upper plate). When the two plates were sealed, the positioning pin was installed in the positioning hole of the upper plate as shown in Figure 6, so as to play a fixed role of the collar of the diving suit.

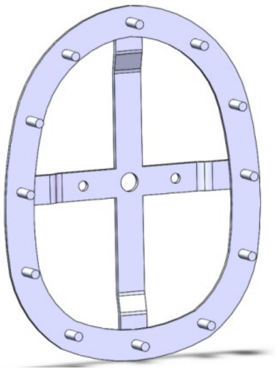

Fig. 6 Combination Diagram of Lower Sealing Ring and Cross Support

As the primary force component of this airtightness testing device, the size of the deformation of the central part of the cross support dramatically affects the reliability of the seal. With a view to avoiding unnecessary waste caused by the production, a preliminary static analysis was conducted by ANSYS, which is a common analysis software, to verify whether the maximum deformation complies with the clamping and sealing requirements. The ANSYS software was used for the static analysis of the support structure, whereby the 3D model of the support structure was imported into the software for the meshing, which is illustrated in Figure 7.

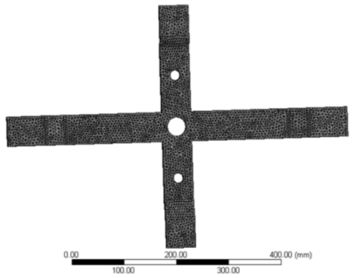

Fig. 7 Meshing Diagram

The faces around the support structure were fixed to emulate the connection with the lower sealing ring. The material selected for the support structure was plain steel, while this material property was assigned to the cross support structure in the software. A force of 1300N was applied at the center circle to emulate the actual force of the support structure in clamping the rubber of the collar of the diving suit. Following the completion of the above settings, the displacement deformation diagram was selected. The displacement cloud diagram of the support structure was obtained by running the calculation, which is presented in Figure 8.

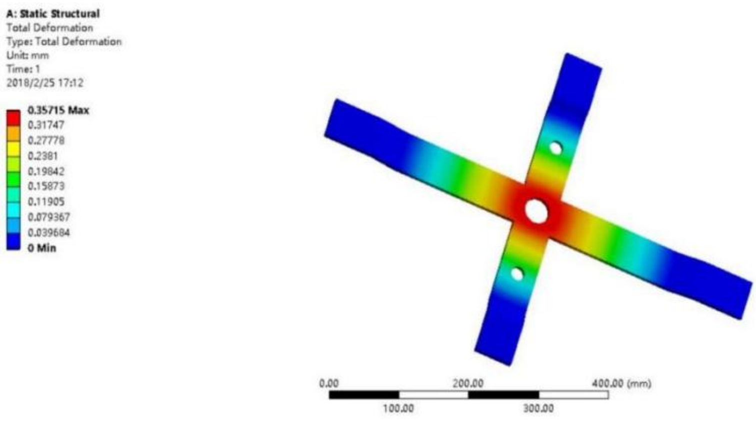

Fig. 8 Displacement Cloud Diagram of Support Structure

As can be obtained from Figure 8, the maximum displacement of the support structure under the condition of 1300N of force in the support structure occurs in the center of the force out, with the maximum deformation displacement of 0.35715mm. In accordance with the design data, it can be concluded that the center of the support frame is far greater than the maximum deformation displacement of the bracket from the outer plane of the lower plate circle, which means that the design complies with the use requirements.

(3) Design of Support Guide Groove

When the cylinder drives the movement of the lower plate by means of the piston rod, since the area of the sealing plate is overly large and the piston rod is partially gravitated by the gravity of the lower sealing plate and the diving suit, the adoption of the piston rod of φ26 fails to keep the movement of the two plates stable. For this reason, it is necessary to install a stabilizing device on the movement trajectory of the sealing plate, so as to keep the plate movement process stable and ensure the sealing of the plate. There are various positioning devices available in modern factories, from which the most suitable guide groove for actual production needs was selected for this design. In comprehensive consideration of the guide groove installation and actual process operation, the SRB12-300 cylindrical guide was selected, with the end of the guide machined with M8×1.5 fine threads, while the three-dimensional model of the clamping mechanism is now established as illustrated in Figure 9.

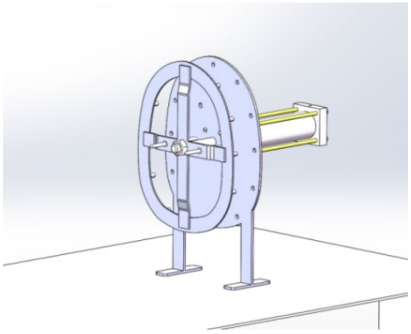

Fig. 9 Three-dimensional Diagram of the Clamping Mechanism

MATHEMATICAL MODELING AND ANALYSIS OF PNEUMATIC SERVO CONTROL SYSTEM FOR AIRTIGHTNESS EXPERIMENT DEVICE

Supposed Conditions

The model of the proportional valve-controlled cylinder was simplified as illustrated in Figure 10. Given the exclusive characteristics of the gas, the following assumptions were made to establish the mathematical model of the pneumatic servo system: (1) the air is an ideal gas that satisfies the equation of state of the ideal gas; (2) the movement process of the cylinder piston is an isentropic process; (3) the pressure and temperature of the gas source is constant; the thermal process of the gas in the cylinder chamber is a quasi-static process; (4) the impact of leakage on the system is overlooked; the pipe resistance and pipe flexibility are overlooked.

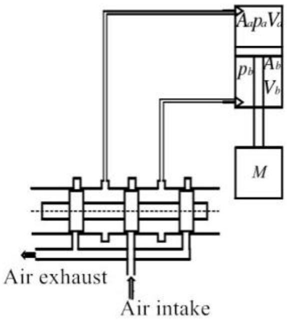

Fig. 10 Simplified Model of Valve-controlled Cylinder

Cylinder Two-chamber Flow Equation

In accordance with the law of conservation of mass: assuming a continuous working medium, the mass flow rate of the gas flowing into and out of the closed volume in a fixed closed volume should be equivalent to the rate of change of the mass of the closed volume, with the following pressure-flow equation:

$$q_{m_b} = \frac{dm_b}{dt} = \frac{d(\rho_b V_b)}{dt} = \rho\frac{dV_b}{dt} + V_b\frac{d\rho_b}{dt} \tag{1}$$

The equation of state of the ideal gas is:

$$\rho_b = \frac{p_b}{RT_b} \tag{2}$$

By combining the above equations, it is obtained that:

$$q_{mb} = \frac{1}{RT_b}\left(p_b\frac{dV_b}{dt} + V_b\frac{dp_b}{dt} - \frac{P_bV_b}{T_b}\frac{dT_b}{dt}\right) \tag{3}$$

In the equation:
Tb -- gas temperature in chamber b of the cylinder (K);
R -- Gas Constant (J/(kg·K));
ρ_b -- Compressed Gas Density(kg/m^3)

In accordance with the initial assumptions, during the process of cylinder filling and deflating, the temperature Ta and the initial temperature Ts satisfy the isentropic adiabatic process, which leads to the following:

$$T_b = T_s\left(\frac{p_b}{p_s}\right)^{\frac{k-1}{k}} \tag{4}$$

In the equation: k -- gas adiabatic index, $k = 1.4$

By taking the derivative of equation (4) with respect to time, it is obtained that:

$$\frac{dT_b}{dt} = \frac{k-1}{k}\frac{T_b}{p_b}\left(\frac{dp_b}{dt}\right) \tag{5}$$

By introducing this into the pressure-flow equation, it is obtained that:

$$q_{mb} = \frac{1}{RT_bk}\left(V_b\frac{dp_b}{dt} + kp_b\frac{dV_b}{dt}\right) \tag{6}$$

The equation (6) is the expression of the gas dynamic process in the b chamber of the cylinder, within the brackets on the right side of the equation, the first term refers to the mass flow rate of the control body being compressed, while the second term refers to the mass flow rate required to change the volume of the control body. The linearization of equation (6) gives that:

$$q_{mb} = \frac{1}{RT_bk}\left(kp_{bi}\dot{V}_b + V_{0b}\dot{p}_b\right) \tag{7}$$

It is assumed in equation (7) that $(\dot{p}_b) = 0$;

When the pressure gas flows into chamber b, the cylinder piston moves to the left, which gives that:

$$V_b = V_{0b} + A_b y \tag{8}$$

It gives that: $\dot{V}_b = A_b\dot{y}$

In the equation (8):
A_b-- the effective area of the piston on the side of the chamber b of the cylinder;

y -- displacement of the piston of the cylinder

$$\Delta q_{mb} = \frac{1}{RT_s k}(V_{0b}\dot{p}_b + kp_{bi}A_b\dot{y}) \quad (9)$$

The gas in chamber a is the outflow, the research is performed for chamber a. In the same way, the mass flow equation of chamber a can be obtained as:

$$-q_{ma} = \frac{1}{RT_a k}\left(kp_{ai}\dot{V}_a + V_{0a}\dot{p}_a\right) \quad (10)$$

When the gas flows out of chamber a, there is:

$$V_a = V_{0a} - A_a y \quad (11)$$

It gives that: $\dot{V}_a = -A_a\dot{y}$

By taking into the equation, it is obtained that:

$$-\Delta q_{ma} = \frac{1}{RT_s k}(V_{0a}\dot{p}_a - kp_{ai}A_a\dot{y}) \quad (12)$$

At the initial time, the piston rod is not subjected to force, it can be concluded that:

$$A_a p_{ai} = A_b p_{bi} \quad (13)$$

By making $\frac{A_b}{A_a} = n$, followed by $p_{ai} = np_{bi}$; where p_{ai}, p_{bi} are the initial steady-state pressures in the chambers of a and $b$respectively.

Given that the initial volume ratio of the two chambers of the cylinder is m

$$m = \frac{V_{0b}}{V_{0a}} \quad (14)$$

Namely: $V_{0a} = mV_{0b}$

By taking the above relationship into the equation, it is obtained that:

$$-\Delta q_{ma} = \frac{1}{RT_s k}\left(\frac{1}{m}V_{0b}\dot{p}_a + kp_{bi}A_b\dot{y}\right) \quad (15)$$

In accordance with the law of conservation of mass: therefore, the storage rate of the mass of the control body is:

$$\Delta q_m = \Delta q_{mb} - \frac{m}{n}\Delta q_{ma} \quad (16)$$

The above modeling calculations have neglected the effect of cylinder leakage.

Equilibrium Equation of Cylinder Piston Force

The effects of Coulomb friction and other nonlinear loads and air will be neglected in the modeling process of this paper. According to the equilibrium equation of cylinder piston force, it is obtained that:

$$A_b P_b - A_a P_a = M\frac{d^2y}{dt^2} + B_f\frac{dy}{dt} + F_L \quad (17)$$

According to the previous relationship, it can be concluded that:

$$A_b(P_b - \frac{1}{n}P_a) = M\frac{d^2y}{dt^2} + B_f\frac{dy}{dt} + F_L \quad (18)$$

In the equation:
M -- cylinder piston and inertia load mass (kg);
FL -- cylinder external load force (N);
B_f -- cylinder internal gas damping coefficient ($\frac{N\bullet s}{m}$).

Proportional Valve Port Pressure -- Flow Analysis

It is assumed that the flow process of the gas through the valve port is considered as a one-dimensional isentropic flow of an ideal gas through a constricted nozzle, which is based on the Sanvile flow equation:

$$q_m = \begin{cases} AP_s x\sqrt{\frac{k}{RT}\frac{2}{k-1}}\sqrt{\left(\frac{P_e}{P_s}\right)^{\frac{2}{k}} - \left(\frac{P_e}{P_s}\right)^{\frac{k+1}{k}}}, 0.528 < \frac{P_e}{P_s} \le 1 \\ AP_s x\left(\frac{2}{k+1}\right)^{\frac{1}{k-1}}\sqrt{\frac{2k}{RT(k+1)}}, 0 < \frac{P_e}{P_s} \le 0.528 \end{cases} \quad (19)$$

In the equation:
α -- flow coefficient of the gas throttle port, where $\alpha = 0.628$ is taken;
A -- effective opening area of the valve orifice (mm^2), where x is the displacement of the spool, and $A = \pi d$ is the area gradient of the valve;

T -- absolute temperature (K);

Pα, Ps -- absolute pressure (MPa);

Given the above two equations, they can be written as a functional relationship as follows:

$$\begin{cases} q_{ma} = f(x, p_a) \\ q_{mb} = f(x, p_b) \end{cases} \quad (20)$$

The linearization of equation (20) by Taylor's formula gives the pressure-flow characteristics near the zero position of the valve port as follows:

$$\begin{cases} \Delta q_{ma} = Kca_{a_{ma}} \\ \Delta q_{mb} = K_{m\,b}x - K_{cb}p_b \end{cases} \quad (21)$$

of which

$$K_{ma} = \left.\frac{\partial q_{ma}}{\partial x}\right| \begin{matrix} x = 0 \\ p = p_a \end{matrix}, \quad K_{mb} = \left.\frac{\partial q_{mb}}{\partial x}\right| \begin{matrix} x = 0 \\ p = p_b \end{matrix},$$

$$K_{ca} = -\left.\frac{\partial q_{ma}}{\partial p}\right| \begin{matrix} x = 0 \\ p = p_a \end{matrix}, \quad K_{cb} = -\left.\frac{\partial q_{mb}}{\partial p}\right| \begin{matrix} x = 0 \\ p = p_b \end{matrix},$$

With the valve spool in the zero position $p_a = p_b$, it can be derived that $K_{ca} = K_{cb} = K_c = 0$.

Transfer Function of Valve-Controlled Cylinder Power Mechanism

According to the above equations (20) and (21), it is obtained that:

$$\frac{m}{n}\Delta q_{ma} + \Delta q_{mb} = \left(\frac{m}{n}K_{ma} + K_{mb}\right)x - \frac{m}{n}K_{ca}p_a - K_{cb}p_b = \left(\frac{m}{n}K_{ma} + K_{mb}\right)x - K_{cb}\left(p_b - \frac{1}{n}p_a\right) - \left(\frac{m}{n}K_{ca} + \frac{1}{n}K_{cb}\right)p_a \quad (22)$$

Given by the assumption: $T_a = T_b = T_s$, it is obtained from equation (22) that:

$$\Delta q_{mb} - (-\frac{m}{n}\Delta q_{ma}) = \frac{1}{RT_s k}(V_{0b}\dot{p}_b + kp_{bi}A_b\dot{y}) - \frac{m}{n}\frac{1}{RT_s k}\left(\frac{1}{m}V_{0b}\dot{p}_a + kp_{bi}A_b\dot{y}\right) =$$

$$\frac{1}{RT_sk}\left[kp_{bi}A_b\dot{y}\left(1+\frac{m}{n}\right)+V_{0b}\left(\dot{p}_b-\frac{1}{n}\dot{p}_a\right)\right] \quad (23)$$

According to $A_a p_{ai}=A_b p_{bi}$, $\frac{A_b}{A_a}=n$, $m=\frac{V_{0b}}{V_{0a}}$, by making $P_{Lb}=P_b-\frac{1}{n}P_a$ and equation (23), it is obtained that:

$$\frac{1}{RT_sk}\left[kp_{bi}A_b\dot{y}\left(1+\frac{m}{n}\right)+V_{0b}\dot{p}_{Lb}\right]=\left(\frac{m}{n}K_{ma}+K_{mb}\right)x-K_{cb}\left(p_b-\frac{1}{n}p_a\right)-\left(\frac{m}{n}K_{ca}+\frac{1}{n}K_{cb}\right)p_a \quad (24)$$

By rectifying and transforming by Laplace, it is obtained that:

$$\left[K_{cb}+\frac{V_{0b}s}{RT_sk}\right]p_{Lb}=\left(\frac{m}{n}K_{ma}+K_{mb}\right)x(s)-\left(\frac{m}{n}K_{ca}+\frac{1}{n}K_{cb}\right)p_a(s)-\frac{1}{RT_s}p_{bi}A_bs\left(1+\frac{m}{n}\right)y(s) \quad (25)$$

Following the Laplace transformation, it is obtained that:

$$A_bp_{Lb}=Ms^2+B_fs+F_L(s) \quad (26)$$

According to the equations (25), (26), the square diagram 11 of the power mechanism diagram of the valve-controlled cylinder.

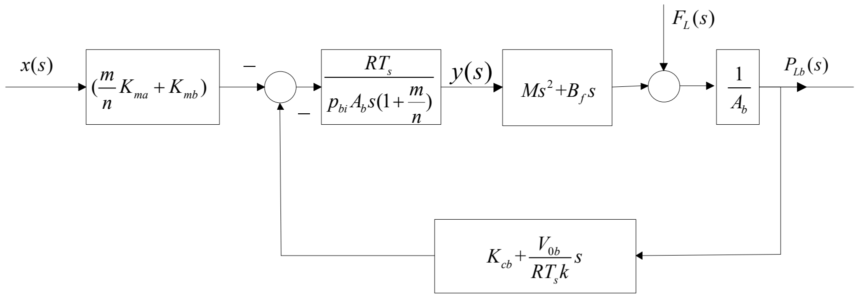

Fig. 11 Square Diagram of the Power Mechanism of Valve-controlled Cylinder

The transfer function of the spool displacement and the load pressure can be derived as:

$$\frac{p_{Lb}(s)}{x(s)}=\frac{A_1s+A_0}{a_3s^2+a_2s+a_1} \quad (27)$$

of which

$$a_1=\frac{p_{bi}(1+\frac{m}{n})}{RT_s},\quad a_2=\frac{MK_c}{{A_b}^2}+\frac{V_{0b}B_f}{RT_skA_b{}^2},$$

$$a_3=\frac{MV_{ob}}{kP_{bi}A_b{}^2}+\frac{B_fK_c}{A_b{}^2}, A_1=\left(\frac{m}{n}K_{ma}+K_{mb}\right)M,$$

$$A_0=\left(\frac{m}{n}K_{ma}+K_{mb}\right)B_f$$

The simplification of the above transfer function gives that:

$$\frac{p_{Lb}(s)}{x(s)}=\frac{\frac{(\frac{m}{n}K_{ma}+K_{mb})RT_s}{(1+\frac{m}{n})A_bp_{bi}}(Ms+B_f)}{\frac{s^2}{{\omega_h}^2}s^2+\frac{2\xi_h}{\omega_h}s+1} \quad (28)$$

In the equation:

$$\omega_h=\sqrt{\frac{(1+\frac{m}{n})kp_{bi}{A_b}^2}{mV0b}}$$

--------pneumatic inherent frequency (radians/s)

$$\xi_h=\frac{K_cRT_s}{2A_bp_{bi}}\sqrt{\frac{Mkp_{bi}}{(1+\frac{m}{n})V_{0b}}}+\frac{B_f}{2A_b}\sqrt{\frac{V_{0b}}{(1+\frac{m}{n})kp_{bi}M}}$$

-------------------------pneumatic damping ratio

Mathematical Model of Proportional Servo System

The block diagram of the servo control system of the diving suit airtightness experimental device is presented in Figure 12:

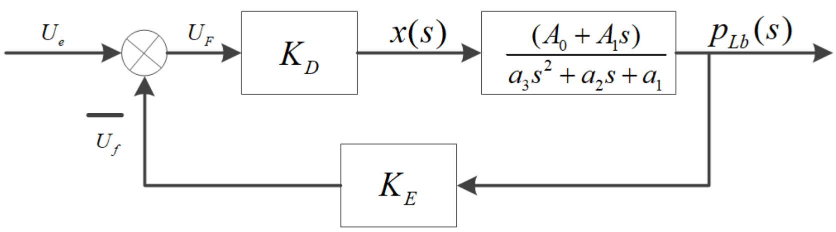

Fig. 12 Block Diagram of the General Model of the Servo System of the Diving Suit Airtightness Experiment Device

$$G(s)=\frac{K(A_0+A_1s)}{a_3s^3+a_2s^2+a_1s} \quad (29)$$

In the equation: $K=K_DK_E$, K_E is the amplification coefficient of the pressure sensor.

In accordance with the structural parameters of the main components and the parameters of the relevant test conditions, the mathematical model of the real system can be derived. The real data of the relevant parameters are presented in Table 1.

Table 1 Real Parameters of the System

No.	Name	Symbol	Unit	Value
1	Cylinder Diameter	D	m	0.1
2	Piston Rod Diameter	d	m	0.02
3	Piston Effective Stroke	L	m	0.16
4	Effective Area of Piston with Rod Chamber	Ab	m2	0.0301
5	Area of Piston without Rod Chamber	Aa	m2	0.0314
6	Initial Pressure with Rod Chamber	pb	MPa	0.34
7	Initial Pressure without Rod Chamber	pa	MPa	0.1
8	Initial Volume with Rod Chamber	Vb0	m3	9.03*10-4
9	Initial Volume without Rod Chamber	Va0	m3	1.26*10-3
10	Nominal Diameter of Valve Port of Proportional Servo Valve Port	d0	m	0.003
11	Spool Diameter	d1	m	0.013
12	Air Adiabatic Coefficient	k		1.4
13	Gas Constant	R	J/(kg·K)	287.1
14	Air Source Pressure	ps	MPa	0.8
15	Operating Pressure	pbi	MPa	0.5

By combining the above parameters, the real model of the servo system can be derived as:

$$G(s) = \frac{10s+11020}{s^3+1080s^2+62.3s} \tag{30}$$

The closed-loop expression of the control system of the diving suit airtightness experiment device is:

$$G(s) = \frac{10s+11020}{s^3+1080s^2+72.3s+11020} \tag{31}$$

Stability Analysis of Servo Control System of Diving Suit Airtightness Testing Experiment Device

In this paper, the Bode diagram method is used to judge the stability of the system according to the phase margin and amplitude margin. According to the requirements, it can be determined that the system is stable when both are greater than zero.

The Bode diagram method is used to analyze the servo control system of the diving suit airtightness experiment device, and the MATLAB programming technology is used. According to the transfer function of the servo control system of the diving suit experimental device, the MATLAB program is written as follows:

```
Num=[10,11020];
Den=[1,1080,72.3,11020];
[mag,phase,w]=bode (num,den);
Margin (mag,phase,w)
```

After running the above program, the following Bode diagram is output:

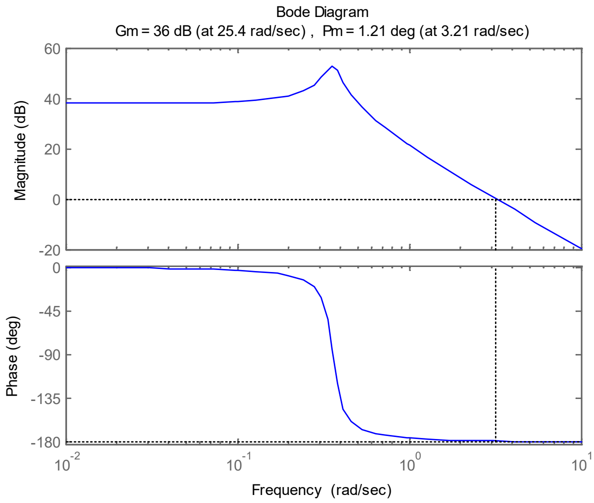

Fig. 13 Bode Diagram of Pneumatic Servo Control System of Diving Suit Airtightness Testing Experiment Device

From the above figure, it can be derived that the servo control system amplitude margin and phase angle margin of this testing experiment device, Gm=36db,Pm=1.21deg, with both values greater than zero, thereby judging that the servo control system of this testing experiment device enjoys excellent stability.

Pole Configuration of Pneumatic Servo Control

System for Diving Suit Airtightness Testing Experiment Device

(1) The transfer function of the servo control system of the diving suit airtightness testing experiment device is:

$$G(s) = \frac{p_{Lb}(s)}{x(s)} = \frac{10s+11020}{s^3+1080s^2+72.3s+11020} \quad (32)$$

The numerator and denominator of equation (32) are multiplied by $\frac{1}{s^3}$, which can be simplified to obtain that:

$$p_{Lb}(s) = x(s)\frac{10s^{-2}+11020s^{-3}}{1+1080s^{-1}+72.3s^{-2}+11020s^{-3}} \quad (33)$$

Assuming that:

$$E(s) = x(s)\frac{1}{1+1080s^{-1}+72.3s^{-2}+11020s^{-3}} \quad (34)$$

It is obtained that:

$$p_{Lb}(s) = 10s^{-2}E(s) + 11020s^{-3}E(s)$$

According to the equation (32), (33), it can be derived the simulation structure diagram of the servo control system of the diving suit airtightness testing experiment device.

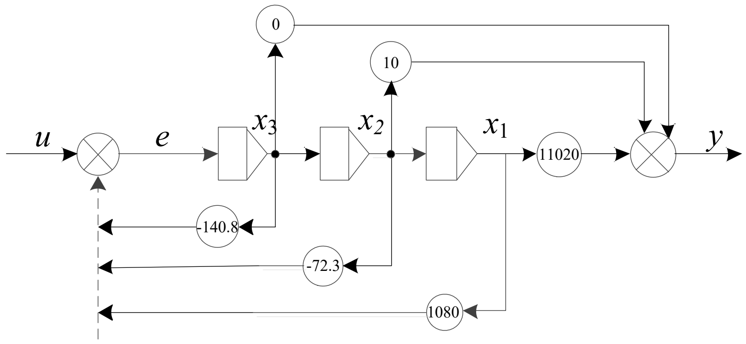

Fig. 14 Structure Diagram of Simulation System

The expression of the state space is derived from Figure 14 as

$$\begin{bmatrix}\dot{x}_1\\ \dot{x}_2\\ \dot{x}_3\end{bmatrix} = \begin{bmatrix}-1080 & -72.3 & -11020\\ 1 & 0 & 0\\ 0 & 1 & 0\end{bmatrix}\begin{bmatrix}x_1\\ x_2\\ x_3\end{bmatrix} + \begin{bmatrix}1\\ 0\\ 0\end{bmatrix}u$$

$$y = [0 \quad 10 \quad 11020]\begin{bmatrix}x_1\\ x_2\\ x_3\end{bmatrix}$$

MATLAB was employed to analyze the state of the servo control system of the diving suit airtightness test device, while the results of the program operation revealed that the results of the closed-loop state space of the pneumatic servo control system of the diving airtightness test device were consistent with the theoretical derivation.

In the study of the pole configuration algorithm for the servo control system of the diving suit airtightness testing experiment device, the sufficient condition for the closed-loop poles to be located at any set position is that the system is completely controllable. The MATLAB was employed to verify that the rank of both the energy observability and controllability matrices of this model were equal to 3, which was equal to its system order, making it possible to determine that the system was controllable. A review of the literature revealed that a set of ideal poles for the third-order transfer function are: $\lambda^*_1 = 387.3$, λ^*_2=0.7, λ^*_3=2400. The state feedback gain matrix K of the system is derived at the given ideal poles.

$$det(sE-A) = \begin{bmatrix} s & -1 & 0\\ 0 & s & -1\\ 11020 & 72.3 & s+1080\end{bmatrix} = s^3 + 1080s^2 + 72.3s + 11020$$

the solution gives:

$$a_1 = 140.8, a_2 = 72.3, a_3 = 1080$$

$$(s-\lambda^*_1)(s-\lambda^*_2)(s-\lambda^*_3) = (s-387.3)(s-0.7)(s-2400)$$

$$= s^3 - 2788s^2 + 928111.11s + 650664$$

the solution gives:

$$a_1{}^* = -2788,\ a_2{}^* = 928111.11,\ a_3{}^* = 650664$$

$$\widetilde{K} = [a_3{}^* - a_3 \quad a_2{}^* - a_2 \quad a_1{}^* - a_1] = [649584 \quad 928038.81 \quad -2928.8]$$

$$Q = [b \quad Ab \quad A^2b]\begin{bmatrix}a_2 & a_1 & 1\\ a_1 & 1 & 0\\ 1 & 0 & 0\end{bmatrix}$$

$$= \begin{bmatrix}0 & 0 & 1\\ 0 & 1 & 140.8\\ 1 & -140.8 & 19752.43\end{bmatrix}\begin{bmatrix}a_2 & a_1 & 1\\ a_1 & 1 & 0\\ 1 & 0 & 0\end{bmatrix} = \begin{bmatrix}1 & 0 & 0\\ 281.6 & 140.8 & 0\\ 0.09 & 0 & 1\end{bmatrix}$$

$$P = Q^{-1} = \begin{bmatrix}1 & 0 & 0\\ 281.6 & 140.8 & 0\\ 0.09 & 0 & 1\end{bmatrix}^{-1} = \begin{bmatrix}1 & 0 & 0\\ -2 & 0.0071 & 0\\ -0.09 & 0 & 1\end{bmatrix}$$

$$K = \widetilde{K}P = [649584 \quad 928038.81 \quad -2928.8]\begin{bmatrix} 1 & 0 & 0 \\ -2 & 0.0071 & 0 \\ -0.09 & 0 & 1 \end{bmatrix}$$
$$= [565649.9 \quad 6589.07 \quad -2928.8]$$

(2) System After Pole Optimization of Pneumatic Servo Control System for Diving Suit Airtightness Test Device

According to the ideal pole, the solved state feedback gain matrix is:

$$K = [565649.9 \quad 6589.07 \quad -2928.8]$$

Its feedback coefficient $k_0 = 565649.9$，$k_1 = 6589.07, k_2 = -2928.8$ is obtained, while the state diagram after the pole configuration is illustrated in Figure 15.

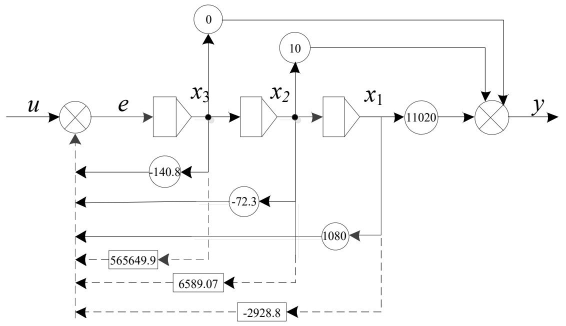

Fig. 15 Structure Diagram of the Closed-loop System after Pole Configuration

Following the optimization of the system, the performance of the two systems was analyzed by comparing the simulation of the original system and the optimized system with a sine wave signal as the input signal, while the simulation diagram of the system is illustrated in Figure 16 and Figure 17.

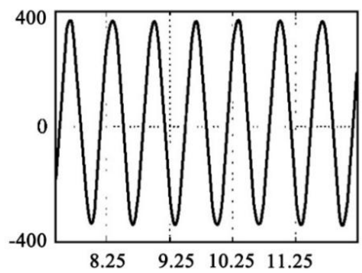

Fig. 16 Simulation Diagram of the Original System

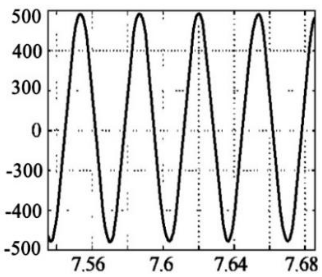

Fig. 17 Simulation Diagram of the System after Optimization of Pole Configuration

Following the pole configuration, the performance of the pneumatic servo system of the diving suit airtightness testing experiment device was significantly improved [17]. This is primarily manifested in the fact that the maximum input of the designed system was 500, and the maximum output of the original system was less than 400 as derived from Figure 16. Following the pole configuration, the maximum input of the system was close to 500 as indicated by Figure 17.

PID Control and Simulation of Pneumatic Servo Control System for Diving Suit Airtightness Testing Experiment Device

With respect to the servo control system of the diving suit airtightness testing experiment device, the simulation model of the control system was established in the simulink module of MATLAB software, which is illustrated in Figure 18.

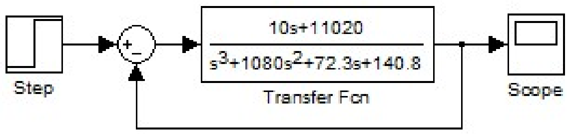

Fig. 18 Simulation Model of Pneumatic Servo Control System of Diving Suit Airtightness Testing Device

Upon running this simulation model, the response diagram of the pneumatic servo control system of the diving suit airtightness testing experiment device was obtained, which is illustrated in Figure 19.

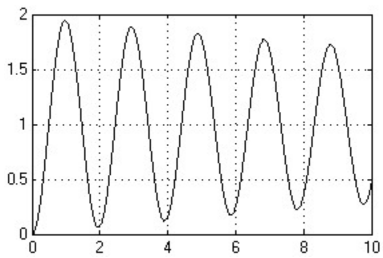

Fig. 19 Simulation Diagram of Pneumatic Servo Control System of Diving Suit Airtightness Testing Experiment Device

It can be concluded from Figure 19 that without optimization, the pneumatic servo control system of the diving suit airtightness testing experiment device experienced oscillations and could not be stabilized in its operation, while there was also a remarkably large amount of overshoot. In view of these issues, the control system needs to be optimized with suitable algorithms.

In various control systems, the control strategy of digital PID has been extensively employed. The components of PID controller can be divided into the following three modules :

(1) Proportional link (P) : Its main function is to reduce the deviation according to the deviation signal of the control system.
(2) Integral link (I) : Its main function is to eliminate static error. After the system is controlled by integral, as long as the time is enough, the control can completely eliminate the steady-state error of the system and improve the control accuracy of the system.
(3) Differential link (D) : The control system is controlled in advance. This method can reduce the deviation of the system adjustment process, reduce the overshoot of the system, overcome the oscillation, and optimize the dynamic performance of the system.

In this paper, the PID parameters were adjusted by experimental trial-and-error method. This method is based on the established system by continuously adjusting the parameters, observing the response under different parameters, and repeatedly adjusting until the response results meet the requirements. In accordance with the mathematical model of the servo control system, the PID control model of the pneumatic servo control system of the diving suit airtightness testing experiment device was established in the simulink module as shown in Figure 20.

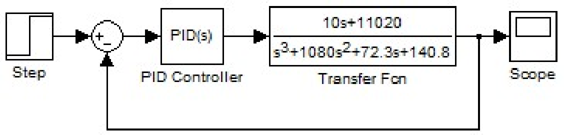

Fig. 20 Simulation Diagram of Pneumatic Servo Control System of Diving Suit Airtightness Testing Experiment Device after PID Control

The values of the parameters for the PID are shown in Table 2.

Table 2 Table of PID Parameter Values

No.	P	I	D
1	25	0	0
2	1	0	0
3	5	0	0
4	9.6	0	0
5	9.6	0.1	0
6	9.6	2	0
7	9.6	0	0.1
8	9.6	0	10
9	9.6	0	5
10	9.6	0	1
11	9.6	0	2.1

By introducing the above taken values into the established PID control model, the images were derived and some of them are as follows:

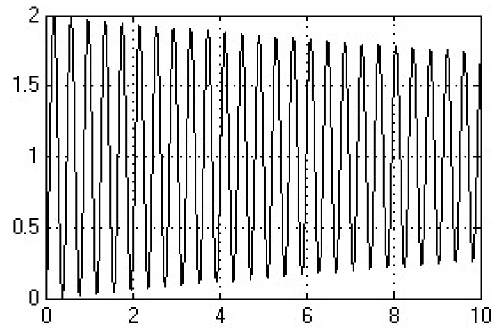

Fig. 21 PID Simulation Diagram of Group 1

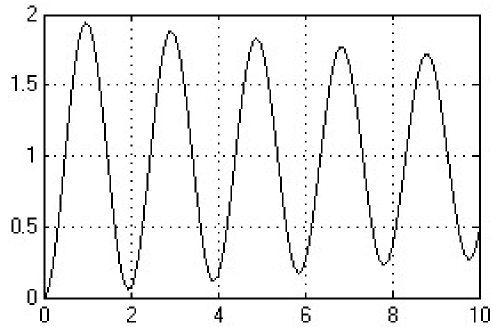

Fig. 22 PID Simulation Diagram of Group 2

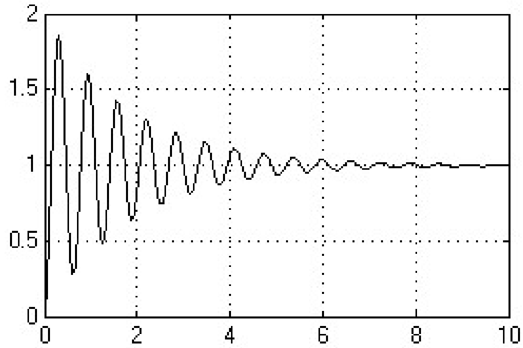

Fig. 23 PID Simulation Diagram of Group 7

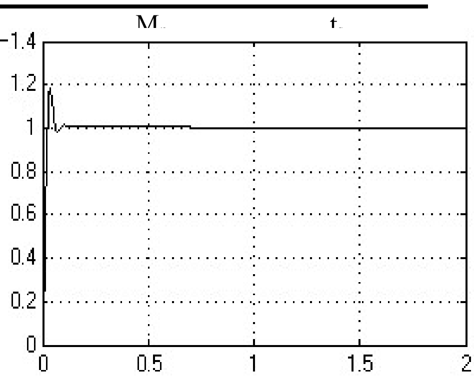

Fig. 24 PID Simulation Diagram of Group 8

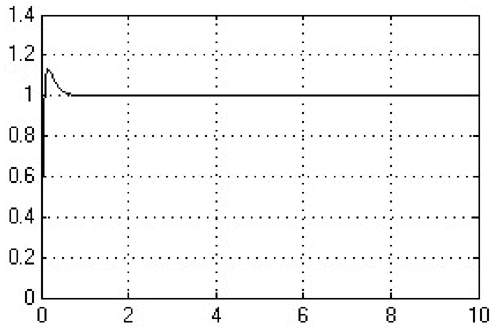

Fig. 25 PID Simulation Diagram of Group 11

By the comprehensive comparison of the simulation diagram of each group, it was concluded that when P=9.6, I=0, D=2.1, the overshoot of the system after PID regulation of the pneumatic servo control system of the diving suit airtightness testing experiment device was significantly reduced, while the output signal of the pneumatic servo control system of the diving suit airtightness testing experiment device reached stability within 1.5 seconds. in this way, it can be concluded that after the introduction of PID control, the overshoot and stabilization time of the pneumatic servo control system of the diving suit airtightness testing experiment device were greatly reduced, which enabled the system to run in a smooth manner.

DESIGN OF AIRTIGHTNESS DETECTION SYSTEM FOR DIVING SUITS

Airtightness detection method

The detection method used in the air tightness detection test device is the direct pressure detection method. The detection method is to fill the constant pressure gas into the inner part of the measured workpiece through the air source, and to form a closed environment inside the measured workpiece through the shutdown of the valve. Then the pressure sensor detects the gas pressure in the measured workpiece. After a period of time, the pressure sensor detects the gas pressure in the measured workpiece again, and observes whether the pressure value of the two tests changes. If the pressure value changes, it indicates that the measured workpiece has gas leakage. The detection principle of the direct pressure detection method is shown in Figure 26. The detection method has the characteristics of fast speed, simple operation and high cost performance.

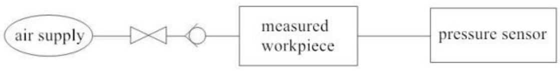

Fig. 26 Direct pressure method detection principle

Leakage derivation for the direct pressure test method

It is assumed that there is no heat exchange in the pressure detection process, it follows from Bomar's law that:

$$P(V_1 - \Delta V_P) = (P - \Delta P)V_1 \qquad (35)$$

In the formula :

P—Detection pressure in diving suit (N) ;

V_1 —The volume of the measured workpiece (m^3) ;

ΔP—Pressure change during pressure detection process (N) ;

ΔV_P—Volume change during pressure detection process (m^3).

The workpieces detected by the direct pressure method are usually in direct contact with the atmosphere. Under this condition, it is concluded that :

$$P_S \cdot \Delta V_S = P \cdot \Delta V_P \qquad (36)$$

After the test time Δt seconds, the amount of gas leakage is :

$$\frac{\Delta V_S}{\Delta t} = \frac{\Delta P V_1}{P_S \cdot \Delta t} \qquad (37)$$

It can be concluded from Formula (37) that the leakage of the measured container can be obtained when the detection time, the atmospheric pressure during the detection, the pressure change of the measured workpiece and the volume of the measured workpiece are known.

The scheme design of the direct pressure detection system

The air tightness test of the diving suit is mainly based on the pressure holding test. When the sealing of the collar, cuff and other parts of the diving suit is completed, the diving suit is filled with compressed gas to make its internal pressure reach 0.01 MPa.After one minute of pressure sensor detection, the pressure is compared with the initial pressure. If the pressure drop is within the standard range, the air tightness of the diving suit meets the design requirements. If it exceeds the standard range, it will alarm the inspector, as shown in Figure 27.

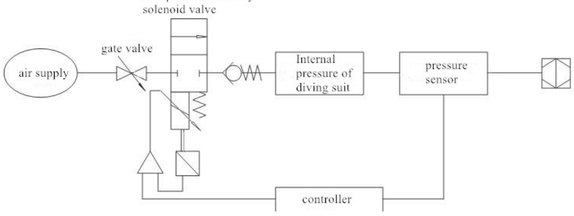

Fig. 27 Diving suit airtightness detection scheme

After the clamping tooling completes the clamping work, the two-position two-way solenoid valve controller obtains the signal to open the diving suit and begin to inflate. When the pressure sensor detects that the air pressure has reached the set air pressure, a signal is issued to close the solenoid valve. After waiting for the air pressure to stabilize, the air pressure change within one minute is detected. The detected data is sent to the controller to compare with the set standard. If the pressure drop exceeds the range, the alarm will be prompted. After the detection is completed, part of the servo valve of the clamping mechanism obtains the signal, releases the pressure, and loosens the diving suit.

Program design based on PLC control

The program design of PLC is the key step to realize the process control of the device, which mainly includes the clamping control of the cylinder, pressure detection, alarm and so on.

(1) Detection process of air tightness of diving suit

When the inspector installs the lower sealing plate and the locating stud of the diving suit into the collar of the wetsuit, open the gate valve and press the start button, the cylinder has a rod cavity to start feeding air and keep the output force of the cylinder unchanged under the control of the servo valve, so that the equipment runs smoothly, when the cylinder starts to compress the rubber, it continues to run until the set clamping force range after the cylinder stops running, the piston stops not moving under the action of the locking circuit. At this time, the two-position two-way valve is opened, and the diving suit begins to inflate. When the sealing detection air pressure is reached, the valve is closed. After the pressure is stable, the pressure detection sensor begins to detect the pressure change after holding the pressure for one minute. When the pressure drop is detected to exceed the set range, the alarm buzzes to remind the inspector that the diving suit sealing does not meet the requirements. Then the diving suit servo valve opens the rodless cavity to start the air intake, and closes the valve after reaching the set position. The inspector closes the gate valve and removes the diving suit.

(2) PLC selection

According to the requirements of the diving control task, the input signal of the air tightness detection platform has 7 inputs and 7 outputs. According to the action requirements of each component of the system and the configuration of the detection device, the model selected in this design is CP1E-NA20DR-A. It is a small application type of relay output type with 20 I / O points connected to AC power supply. The advantage of this design is that it has its own analog input and analog output, and does not require users to expand, fully meets the requirements of this design, and effectively saves the design cost. Under the control of PLC, the diving air tightness detection test device can realize the automation of the detection process. According to the process requirements and operational requirements of the actual detection site, an automatic control flow chart is drawn as shown in Figure 28:

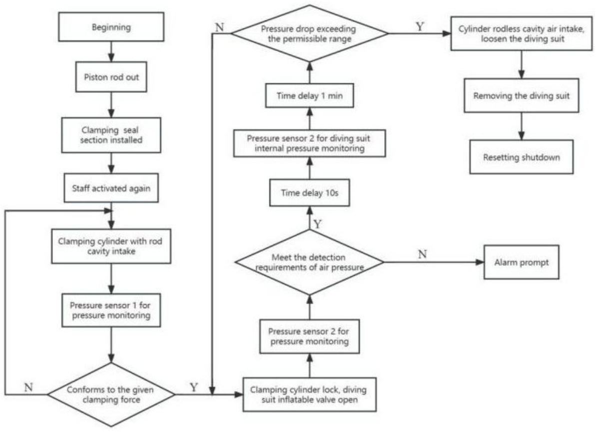

Fig.28 Automatic control process of air tightness detection of diving suit

According to the above detection process, the port allocation of CP1E-NA20DR-A PLC is as shown in table 3.

Table 3 Port allocation table

Serial number	Point position	function	Serial number	Point position	function
1	X0	start-up	8	Y0	clamping cylinder clamping control
2	X1	stopping	9	Y1	clamping cylinder relaxation control
3	X2	emergency stopping	10	Y2	alarm signal
4	X3	cylinder pressure limitation	11	AD0	pressure sensor 1 feedback
5	X4	inflation pressure limitation	12	AD1	pressure sensor 2 feedback
6	X5	clamping cylinder seal complete detection	13	DA0	leakage minimum pressure given
7	X6	inflatable complete detection	14	DA1	sealing force given

CONCLUSION

This paper completed the design of the clamping and sealing module, established the mathematical model of the pneumatic servo control system of the diving suit airtightness testing experiment device, optimized the pneumatic servo control system, in addition to determining the pressure detection scheme of the diving suit airtightness testing experiment device. Meanwhile, the following conclusions are drawn:

(1) In accordance with the requirements of the testing process, the testing device program was designed, the clamping force control program of this testing device with servo control as the core was established, the schematic diagram of the pneumatic system was drawn, the clamping and sealing structure and the overall structure of the air tightness testing device was designed, while ANSYS analysis was performed for the main force components of the sealing device to verify that the deformation of the support structure made of steel as the raw material complies with the clamping requirements.

(2) With the analysis of the valve-controlled cylinder mechanism, the mathematical model of the force-servo control system of the test device was established, while the Bode diagram was obtained by adopting MATLAB software to simulate the system, thereby analyzing the stability of the system. From the Bode diagram, it can be concluded that the amplitude margin and phase angle margin of the servo control system of the test device, Gm=36dB, Pm=1.21deg, both values are greater than zero. As a consequence, the stability of the servo control system of the testing device was determined to be excellent.

(3) By means of simulink, the force-servo control system of the diving suit airtightness testing device was modeled and simulated, which resulted in the step response curve of the system. The optimal control model of the system was obtained by applying the pole configuration and PID algorithm to optimize the force servo control system of the diving suit airtightness testing device. Following the pole configuration, the maximum input of the system approached 500, while the performance of the pneumatic servo system of the diving suit airtightness testing test device was dramatically improved. Following the introduction of PID control, the overshoot and stabilization time of the pneumatic servo control system of the diving suit airtightness testing experiment device were substantially reduced, enabling the system to enter smooth operation as soon as possible.

(4) According to the research of air tightness testing method, the testing scheme of diving suit air tightness testing experiment device was determined, while the control program of PLC was designed in accordance with the whole testing process.

(5)

AUTHOR CONTRIBUTIONS

Guoqing Gong had made substantial contributions to design, experimental research, data collection and result analysis; Youmin Wang made critical changes to important academic content; Peng Gong made the final review and finalization of the articles to be published.

DATA AVAILABILITY

The data used to support the findings of this study are included within the article.

CONFLICTS OF INTEREST

The authors declare that they have no conflicts of interest.

REFERENCES

Alberto Trevisani, Dario Richiedei, Iacopo Tamellin, et al. Pole Assignment for Active Vibration Control of Linear Vibrating Systems through Linear Matrix Inequalities[J]. Applied Sciences, 2020, 10 (16).

Benarab Amina, Boussaada Islam, Niculescu Silviu-Iulian, et al. Over one Century of Spectrum Analysis in Delay Systems: An Overview and New Trends in Pole Placement Methods[J]. IFAC PapersOnLine, 2022, 55 (36).

Bharat S. Patil, Dwarkoba P. Gaikwad, Laxman S. Patil. Advance genetic algorithm-based PID controller for air levitation system[J]. International Journal of Modelling, Identification and Control, 2022, 41 (3).

Chen Dongdong, Fang Lei, Fang Zifan, et al. A proportional servo valve control method based on state feedback[J]. Flight Control and Detection, 2022 5 (1): 39-47.

Claire Jean-Mistral, Shaoyi Zhou, Simon Chesne. Electromagnetic shunt damping with negative impedances: Optimization and analysis[J]. Journal of Sound and Vibration, 2019, 445.

Dang Lifeng, Gu Chiyu. Design of air tightness detection system based on Siemens S7-1200PLC[J]. Agricultural equipment Technology, 2020, 46 (6): 3.

Duan Suolin, Wang Chunling, Zhao Peng, et al. Valve body airtightness detection method based on improved SIFT algorithm[J]. Journal of Changzhou University: natural Science Edition, 2020 (4): 37-45.

Gao Jie, Liu Yang, Zhang Linggai. Application of Weighted Fusion Algorithm in Air Tightness Detection Device[J]. Journal of Physics: Conference Series, 2019, 1187 (3).
Guo Qi, Meng Fanzhe, Wang Han, et al. Experimental study on Predictive Fuzzy PID Control in Atmospheric and vacuum Distillation Unit[J]. Control Engineering, 2020, 27 (9): 1495- 1501.
Jiang Cuicui, Wang Zuoxun. Application of fuzzy-PID control in pressure control system of air tightness detection[J]. Journal of Qilu University of Technology, 2021, 35 (03): 52-58.
Jiang Qing, Wang Qiongpei. Design of leakage detector based on ultrasonic sensor[J]. Instrument Technology and sensors, 2018 (9): 4.
Liao Huguang, Lin Weiguo. Air tightness testing method of pressure vessel based on piezoelectric pressure sensor[J]. Journal of Beijing University of Chemical Technology: natural Science Edition, 2022, 49 (5): 7.
Li Haibin, Su Qi, Zhang Zhihao, et al. Optimal design of low hydraulic power spool diversion structure of proportional servo valve[J]. Flight Control and Detection, 2022, 5 (1): 8.
Li Haoliang, Xi Qian, Yang Rennong, et al. Conformance of time-varying delay multi-agent systems based on distributed PID control[J]. Control and decision-making, 2019, 34 (1): 189-197.
Li Jiansong, Liu Qing, Zhou Bo. Design of automatic testing device for scroll compressor shell based on direct pressure detection method[J]. Machine tool and hydraulic pressure, 2018. 46 (16): 5.
Lu Shan, Rossiter John Anthony, Su Hongye, et al. A low-cost pole-placement MPC algorithm for controlling complex dynamic systems[J]. Journal of Process Control, 2022, 111.
Mao Qibo, Wang Yong, et al. Optimal design of electromagnetic shunt damping based on pole collocation method[J]. Noise and Vibration Control, 2022, 542 (6): 19-23.
Peng Ke. Design of digital pneumatic servo control platform [D]. China University of Mining and Technology, 2021.
Seigo Goto, Shenglin Mu, Satoru Shibata, et al. Intelligent position control for pneumatic servo system based on predictive fuzzy control[J]. Computers and Electrical Engineering, 2019, 75.
Shi Taicheng, Tong Yi, Xiong Yuansheng, et al. Design of air tightness detector for water level sensor based on STM32[J]. Electromechanical Information, 2023 (4): 4.
Wang Boyang, Xu Guiyin, Zhang Shi. Pneumatic servo control method of double solenoid valve based on PPM and proportional control[J]. Digital Communication World, 2022 (005): 000.
Wang Lin. Heat balance analysis of dual fuel engine[D]. Dalian Maritime University, 2020.
Zhao Na. Research on position control of linear cylinder based on proportional directional valve[D]. Lanzhou University of Technology, 2009.

潜水衣气密性实验装置控制性能研究

宮國慶 王幼民 龚鹏

安徽工程大學機械工程學院

摘要

当前潜水装置气密性检测方法较为落后，检测设备操作复杂且效率较低，无法确保每一件潜水衣气密性。针对潜水衣气密性实验装置的基本研发，本文确定了以夹紧力伺服控制为核心的控制方案，使用 Solidworks 绘制了气密性检测装置的夹紧密封模块的三维模型，同时针对主要受力部件进行了 ANSYS 分析。其次建立了潜水衣气密性检测试验装置气动伺服控制系统的数学模型，使用 Matlab 对潜水衣气密性检测试验装置的伺服控制系统进行分析，判断出该检测试验装置的伺服控制系统稳定性良好，通过极点配置后，潜水衣气密性检测试验装置气动力伺服系统的性能得到显著的改善，在引入 PID 控制后潜水衣气密性检测试验装置气动伺服控制系统的超调量和稳定时间都得到了大幅缩减。最后完成了气密性检测方法的研究，利用直压检测法检测原理，确定了潜水衣气密性检测试验装置的检测方案，并根据整个检测流程对 PLC 的控制程序做出了设计。